

Inter-Area Oscillations in Tunisia's 2030 Grid: Insights from Koopman Modal Analysis

Yassine BOUSSAA^{#1}, Khadija BEN KILANI^{#2}, Fethi GHODHBANE^{#3}

[#]Université de Tunis El Manar, ENIT, L.S.E, LR11ES15, BP 37-1002, Tunis le Belvédère, Tunisie,

¹yassine.boussaa@enit.utm.tn

²khadija.kilani@enit.utm.tn

³fathi.ghodbane@enit.utm.tn

Abstract — The large-scale integration of renewable energy sources (RES) is profoundly transforming the dynamic behavior of modern power systems by reducing system inertia and intensifying nonlinear interactions among geographically distributed areas. Conventional eigenvalue-based small-signal stability analysis provides valuable information around operating points but fails to capture hidden nonlinear oscillatory dynamics that emerge under high RES penetration and large disturbances. This chapter investigates the oscillatory stability of the Tunisian power system projected for 2030 under a national peak-load scenario with 35% RES penetration. A detailed nonlinear model implemented in PSAT is employed to perform time-domain simulations. The study combines Classical Linear Modal Analysis (LMA) with Koopman Modal Analysis (KMA), a data-driven operator-theoretic framework capable of extracting coherent spatiotemporal structures directly from system trajectories. Results show that the most critical oscillatory behavior lies within the frequency band [0.5–1.2 Hz], with dominant dynamics concentrated between 0.7 and 1 Hz. The principal Koopman mode at 0.81 Hz exhibits weak damping and long decay time, revealing a strong inter-area oscillation between the Northern region and the combined Central–Southern area. By coupling geographic segmentation with K-means clustering applied to Koopman mode shapes, three coherent dynamic groups are identified, corresponding to inter-area, moderately coupled, and localized oscillations. The findings demonstrate that KMA not only reproduces dominant modes predicted by linear analysis but also uncovers hidden nonlinear components essential for accurate stability assessment. The chapter highlights practical implications for stability enhancement, including optimal tuning of power system stabilizers, reinforcement of inter-area corridors, and deployment of wide-area monitoring systems.

Keywords — Inter-area oscillations; Koopman operator; DMD; non-linear modal analysis; large-scale renewable energy integration; Generators coherency; wide-area monitoring; Tunisian power system.

I. INTRODUCTION

The rapid deployment of renewable energy sources (RES), particularly wind and photovoltaic generation, is fundamentally reshaping power system dynamics worldwide. While these resources contribute to decarbonization and energy sustainability, their increasing penetration displaces conventional synchronous generators, leading to reduced system inertia, weaker synchronizing torque, and higher sensitivity to disturbances [1], [2]. Consequently, modern power grids are becoming more vulnerable to low-frequency electromechanical oscillations, especially inter-area modes that involve large geographical regions.

Traditional stability assessment relies mainly on small-signal analysis based on linearized system models. Although this approach provides valuable insight into dominant oscillatory modes, damping ratios, and participation factors [3], it inherently neglects nonlinear and time-varying phenomena that emerge in renewable-rich power systems, particularly under large disturbances or fluctuating RES output. As a result, important dynamic features may remain hidden, leading to inaccurate risk assessment and suboptimal control strategies.

In recent years, data-driven approaches have gained increasing attention for power system dynamics analysis. Among them, Koopman Modal Analysis (KMA) offers a powerful operator-theoretic framework that enables the representation of nonlinear dynamics through linear evolution in an extended observable space. By directly exploiting time-series data, KMA extracts coherent spatiotemporal structures and reveals nonlinear oscillatory components that are not accessible through classical eigenvalue analysis [4–7].

This chapter focuses on the Tunisian power system projected for the 2030 horizon, characterized by a high penetration of renewable energy sources (35%) and significant north–south power transfers. Using a detailed nonlinear model implemented in PSAT, the study combines Classical Linear Modal Analysis (LMA) and

Koopman Modal Analysis (KMA) to investigate inter-area oscillations under peak-load conditions. The main objectives are to (i) identify dominant oscillatory modes, (ii) reveal hidden nonlinear dynamics, (iii) assess generator coherency patterns, and (iv) derive practical recommendations for stability enhancement.

II. TUNISIAN 2030 POWER SYSTEM AND SIMULATION FRAMEWORK

This section presents the modeling framework and operating scenario adopted to investigate the dynamic behavior of the Tunisian power system projected for 2030.

A. System Modeling and Simulation Framework:

The Tunisian power system projected for 2030 is characterized by substantial structural evolution, including the reinforcement of the high-voltage transmission network, the deployment of new combined-cycle units, and the large-scale integration of renewable energy sources (RES). These developments significantly reshape the dynamic behavior of the grid by altering power-flow patterns, modifying generator dispatch, and reducing overall system inertia. To accurately capture these dynamics, a detailed nonlinear model of the 2030 Tunisian power grid was developed using the Power System Analysis Toolbox (PSAT). The initial network configuration was originally generated with (PSS®E) by the Tunisian Electricity and Gas Company (STEG), then adapted and refined within PSAT to incorporate updated generation capacities, transmission configurations, and operating conditions provided by national planning studies.

B. National Peak-Load Scenario in 2030 with 35% RES Penetration:

The 2030 Tunisian power system consists of a meshed 225–400 kV transmission backbone interconnecting three main geographical zones: the **North**, hosting the Rades thermal and combined-cycle plants (G1–G5) and the BMC Zaghen gas turbines (G6–G7); the **Central** region, dominated by the Sousse C–D combined-cycle units (G10–G12), which play a key role in dynamic support and power balancing; and the **South**, supplied mainly by the Gahrouch combined-cycle plant (G13) and the Bouchemma gas turbine (G14). The list of active synchronous generators and renewable generators considered in the **national peak-load scenario** is summarized in Table 1.

Table 1 – Geographical Distribution of Active Conventional and Renewable Generators in the 2030 Peak Load Scenario

Category	Bus Number	Synchronous Generator Name	Abbreviated Name	P _{MAX} (MW)	Zone	Geographical Map	
Conventional Sources (14 active synchronous generators)	343	TG RDC	G1	450	North		
	344	TV RDC	G2	250			
	333	RADES2 G1	G3	150			
	335	RADES2 CC	G4	471			
	334	RADES2 G2	G5	150			
	345	BMC TG3	G6	120			
	346	BMC TG4	G7	120			
	326	TG CC1 SS	G8	120	Central		
	327	TG CC2 SS	G9	120			
	328	CC SS B	G10	424			
	340	CC_SS C	G11	424			
	341 (Slack Bus)	CC_SS D	G12	424			
	337	CC GHNCH	G13	412	South		
	352	TG3 BCHM	G14	240			
Renewable Energy Sources IRPL ¹ :35%	Wind Power	Photovoltaic Power	Total (Wind + PV)				
	656,39	1469,66	2126,05				
Total Installed Capacity (Conventional + RES)				2126 + 3875 = 6001MW			

The study focuses on the national peak-load operating condition (≈ 6000 MW), where partial displacement of synchronous generation by RES leads to increased North–Centre–South power transfers. Under these

¹ IRPL : Instantaneous Renewable Penetration Level = 35%

conditions, the 400 kV backbone tends to become congested, and the system exhibits heightened sensitivity to inter-area oscillations. Fourteen synchronous generators are modeled using sixth-order machine representations with detailed excitation and turbine-governor dynamics, ensuring accurate capture of electromechanical oscillations. In addition, large-scale wind and photovoltaic (PV) sources are connected at 225 kV and 150 kV levels, contributing to a 35% instantaneous renewable penetration and significantly lowering the system's effective inertia. To excite these dynamics, a three-phase short-circuit fault is applied at the Ezzahra 225 kV bus in the Northern region. The fault, cleared after 200 ms, induces pronounced electromechanical swings and inter-area oscillations. Nonlinear time-domain simulations are performed in PSAT, using a fine time step over a 20-second window, allowing detailed observation of both transient and sustained oscillatory behavior.

III. METHODOLOGY

This section presents the methodological framework used to analyze the oscillatory behavior of the Tunisian 2030 power system. The approach combines Classical **Linear Modal Analysis (LMA)** focused on small-signal stability around the operating equilibrium, a nonlinear **Koopman Modal Analysis (KMA)** providing a global representation of system dynamics, and data-driven coherency assessment through K-means clustering. Together, these methods provide complementary perspectives on the linear and nonlinear mechanisms driving inter-area oscillations under high renewable energy penetration.

A. Workflow of the Renewable Integration Study - Linear and Nonlinear Modal Analysis

The study begins with a steady-state power flow analysis of the base network (without RES) using MATLAB/PSAT to initialize system states. Renewable sources are then progressively integrated by specifying injected power, technology type, and control mode, followed by network rebalancing. Once convergence is achieved, a disturbance is applied and the dynamic response is analyzed. Time-domain simulations are examined from two perspectives: LMA, based on system linearization, extracts conventional eigenmodes, while KMA is applied directly to nonlinear simulated signals without linear approximation. KMA reveals lightly damped modes, nonlinear couplings, and inter-area oscillatory patterns that are not captured by LMA. Results from both analyses are compared to assess modal consistency and stability limits, guiding the acceptable renewable penetration level.

B. THE KOOPMAN OPERATOR FRAMEWORK

1) Koopman operator definition

Koopman Modal Analysis is a data-driven, operator-theoretic approach that represents nonlinear system dynamics through a linear operator acting on observable functions [5]. For a discrete-time nonlinear system, observables derived from simulations or measurements (e.g., generator dynamics or bus voltages) evolve linearly under the Koopman operator, enabling spectral analysis without model linearization [5], [11]. An Arnoldi-type algorithm approximates the Koopman eigenvalues and modes from stacked observable snapshots.

2) Stability of Koopman modes

The performed Mode Decomposition not only provides dimensionality reduction in terms of a reduced set of modes but also sets a model for how these modes evolve in time. The damping ratio of Koopman modes are quantified by their growth rates. The growth rate GR_j [4–14] of the j^{th} Koopman mode is determined by the amplitude of its j^{th} eigenvalue $\tilde{\lambda}_j$.

$$GR_j = \ln |\tilde{\lambda}_j| / \Delta t \quad (1)$$

A smallest growth rate denotes a largest damping ratio. The stability limit of Koopman modes is defined by the unit circle. An unstable Koopman eigenvalue has modulus larger than one. Its corresponding Koopman mode grows exponentially as time increases. A GR less than one involves a damped (stable) Koopman mode. For a given j^{th} Koopman mode, the temporal evolution of its growth rate is given by the j^{th} line of the matrix M , where each of its components M_{jk} is defined by the modulus of the component T_{jk} of the Vandermonde matrix T :

$$M_{jk} = |T_{jk}| \quad (2)$$

The modal vector (mode shape) \mathbf{V}_j , from which the norm $\| \mathbf{V}_j \|$ is extracted, reflects the energetic contribution of the mode to the overall system behavior.

The damping ratio is expressed in percentage as $\zeta_{\text{damping}}(\%)$. It should be noted that the minimum damping ratio must remain above 5%.

The dominance criterion is given by:

$$D_k = GR_j \cdot \| V_j \| \quad (3)$$

which highlights modes that are simultaneously weakly damped and strongly represented in the system observables.

C. Selection of Observables and Data Embedding

A key step in KMA is the selection of observables that capture the essential electromechanical behaviors of the grid. In this work, three categories of observables are used: Rotor speeds $\Omega_i(t)$, Rotor angles $\delta_i(t)$ and Active powers $P_{\text{gen},i}(t)$. Temporal structure is embedded using a Hankel matrix constructed from time-shifted snapshots, allowing the Koopman approximation to capture both transient and sustained oscillatory behaviors across multiple frequencies.

D. Dynamic Mode Decomposition (DMD)

The Koopman operator is approximated using Dynamic Mode Decomposition, which combines singular value decomposition with low-rank operator estimation to extract Koopman eigenvalues, frequencies, growth rates, and mode shapes. DMD is chosen for its robustness and efficiency in capturing nonlinear oscillatory dynamics in power systems [4], [8], [9], [15]. Filtering criteria based on dominance, frequency range (0.5–1.2 Hz), spatial coherence, and physical interpretability are applied to isolate meaningful modes.

E. Generator Coherency Analysis

Generator coherency is analyzed using both manual and automatic approaches. Manual grouping follows the geographical North–Centre–South structure of the Tunisian grid, reflecting physical transmission corridors. In parallel, K-means clustering is applied to Koopman mode shapes to identify coherent generator groups in a fully data-driven manner. The resulting clusters align with the geographical partition while providing refined dynamic insight into inter-area oscillations.

IV. RESULTS

This section analyzes the oscillatory behavior of the Tunisian 2030 grid under peak-load conditions with 35% RES penetration using both LMA and KMA. The combined approach reveals critical linear and hidden nonlinear modes, along with their spatial coherency, providing a comprehensive stability assessment.

4.1 Linear Modal Analysis Results

Linear Modal Analysis (LMA) identifies three dominant inter-area oscillatory modes in the 0.78–0.91 Hz range, characteristic of North–Centre–South interactions in the Tunisian grid. These modes exhibit low damping ratios (3–6 %), clustered frequencies around 0.8–0.9 Hz, and strong participation from Northern generators, particularly the Rades units. Central combined-cycle units contribute moderately, while Southern generators show weaker but coherent participation. Despite correctly identifying the main inter-area mode, the linear nature of LMA limits its ability to capture nonlinear interactions and multi-frequency dynamics, motivating the use of Koopman Modal Analysis to reveal additional nonlinear modes.

4.2 Koopman Spectrum and Frequency Band Decomposition

Koopman Modal Analysis provides a richer spectral description than linear analysis, using rotor speed, rotor angle, and active power as observables, with the Koopman operator approximated via DMD from a Hankel matrix. The filtered Koopman spectrum in the 0–3 Hz range, shown in **Fig. 1**, reveals four dynamic regions: global low-frequency behavior below 0.5 Hz, inter-area oscillations between 0.5 and 1.1 Hz, mainly local modes from 1.1 to 2 Hz, and negligible high-frequency components above 2 Hz. The most critical dynamics are concentrated in the 0.5–1.1 Hz band, particularly around 0.76–0.96 Hz, where several modes exhibit low damping ratios (<5%). The dominant KM mode at 0.81 Hz shows the weakest damping and highest dominance, corresponding to an inter-area oscillation between the Northern and [Central + Southern] regions, potentially leading to persistent oscillations. The distribution of damping ratios within 0.01–1.2 Hz, illustrated in **Fig. 2**, highlights a critical vigilance zone between 0.7 and 1.2 Hz, where weakly damped modes may sustain oscillations following disturbances.

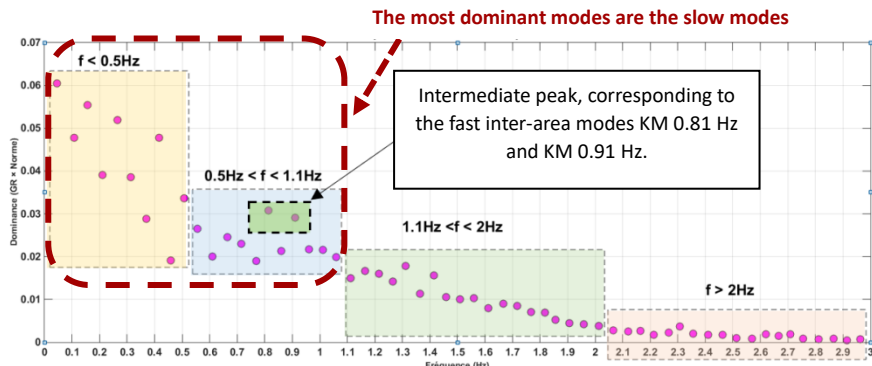


Figure 1: Spectrum of the filtered Koopman modes in the [0–3 Hz] frequency band

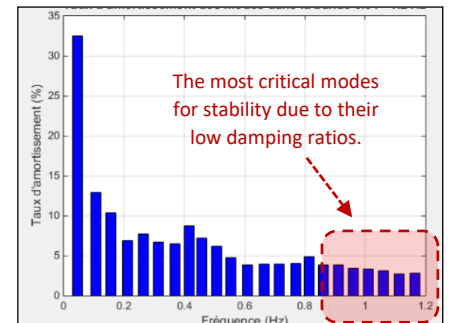


Figure 2: Damping Ratios of Modes in the Inter-Area Oscillation Band

Cross-referencing these results with the damping analysis and the mode-shape examination will help prioritize stability enhancement actions, particularly regarding the network's most sensitive areas.

Generator coherence was analyzed using both manual geographic segmentation (North, Centre, South) and automated K-means clustering of complex modal vectors. Fourteen critical modes within the [0.5–1.2 Hz] band were classified into three topological groups. **Fig. 3** illustrates the Koopman spectrum mapped in the frequency–dominance plane using *manual geographical grouping*, where each mode is represented according to its dominance.

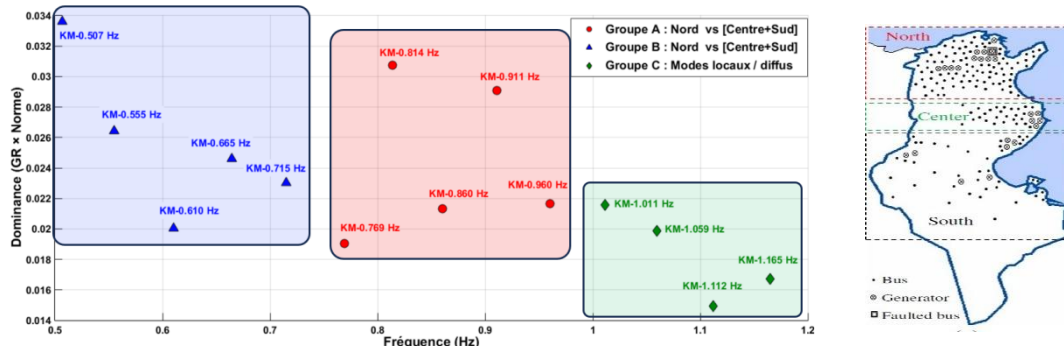


Figure 3: Koopman spectrum in the frequency–dominance plane showing three topological groups

Three topological groups emerge. **Table 2** provides the classification of Koopman modes into three topological groups based on their dominant characteristics and dynamic behavior.

Table 2: Topological Grouping of Koopman Modes in the Critical Frequency Band

Group	Dominant Characteristics	Dynamic Behavior	Included Modes
A	Clear opposition between North vs. [Central + South] , with strong involvement and high coherency of the Northern generators.	Well-structured inter-area modes, showing a distinct decoupling between G1–G7 (North) and G11–G12 (Central) + G13–G14 (South).	KM-0.813 Hz, KM-0.911 Hz, KM-0.961 Hz, KM-0.860 Hz, KM-0.768 Hz
B	Opposition between North vs. [Central + South] , with a highly coherent but moderately involved Northern area.	Inter-area modes with strong participation of G2 and G4 (North), and weak involvement of Central and Southern generators. These modes are less structured but still engage all regions, with the Central area often weakly stressed or dynamically neutral.	KM-0.506 Hz, KM-0.554 Hz, KM-0.664 Hz, KM-0.715 Hz, KM-0.610 Hz
C	Weakly structured or local modes, dominated by a few generators in the Northern area.	Local or broad but weakly organized oscillations, typically centered on the Northern zone and characterized by internal detuning effects.	KM-1.112 Hz, KM-1.165 Hz, KM-1.059 Hz, KM-1.011 Hz

The **mode shapes** associated with the dominant modes, shown in Fig. 4, confirm the existence of clear phase opposition between the Northern and Southern zones, characteristic of large-scale inter-area oscillations. These

spatial patterns are consistent with the physical topology of the 400 kV backbone RADES–SIDI BOUZID–SKHIRA, which constitutes a weak coupling corridor under high renewable penetration. The oscillation pattern of the KM-0.81 Hz mode further emphasizes the need to strengthen this transmission path, particularly through reactive compensation and improved damping control.

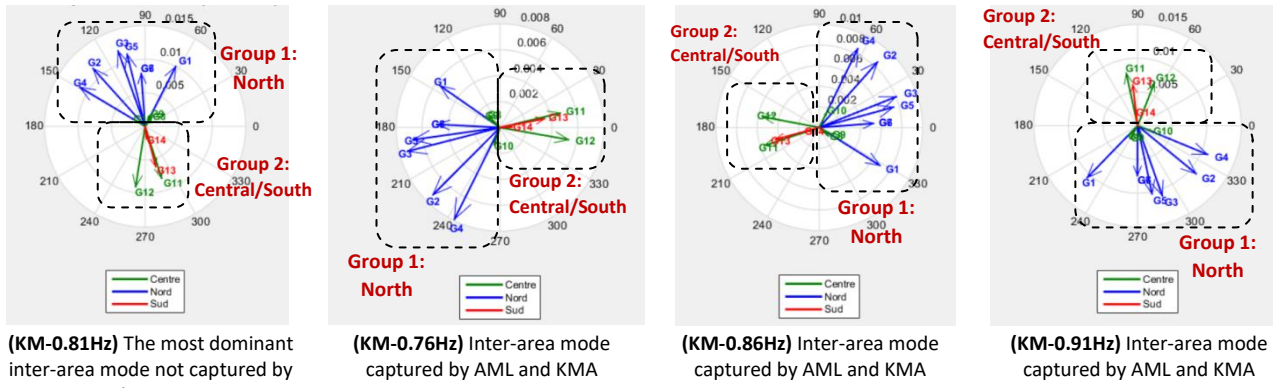


Figure 4: Mode Shapes of the Most Dominant Koopman Modes - manually classified using geographical topology

When compared with classical linear modal analysis, KMA reproduces the main inter-area oscillation near 0.8 Hz but additionally exposes hidden nonlinear modes that are not detected in the small-signal framework. These hidden components reflect nonlinear energy exchanges among synchronous generators and converter-based renewable units, which become more significant in high-RES scenarios.

4.3 Generator Coherency: Manual vs. Data-Driven Clustering

The coherency structure of the Tunisian 2030 system was first examined through a manual geographical grouping based on topological zoning, which naturally separates the generators into three areas: the North (G1–G7), the Centre (G8–G12), and the South (G13–G14). This partition reflects the historical structure of the grid and provides an intuitive baseline for interpreting inter-area oscillations.

A complementary, data-driven analysis was then performed using K-means clustering applied to the Koopman mode shapes. This unsupervised approach automatically classified the oscillatory behavior into three coherent groups that closely match the geographical zoning, while offering a more refined view shaped by the actual dynamic responses. The first cluster (Group A, 0.76–0.96 Hz) captures the dominant inter-area oscillations, where North–South exchanges are most pronounced. The second cluster (Group B, 0.50–0.71 Hz) contains intermediate modes in which the Central region contributes a stabilizing effect. The third cluster (Group C, above 1 Hz) corresponds to localized dynamics essentially confined to the Northern area.

Overall, both manual zoning and data-driven clustering converge to the same structural interpretation: the Northern region emerges as the primary oscillatory source, the Centre behaves as a dynamic buffer between the two extremities of the grid, and the South tends to oscillate coherently with the Centre. These findings are illustrated in **Fig. 5**, which displays the automatic K-means clustering of the Koopman modes. The mode shapes in the critical [0.7–1 Hz] frequency band associated with each cluster were identified and shown to be practically identical to those obtained using the manual coherency-based method.

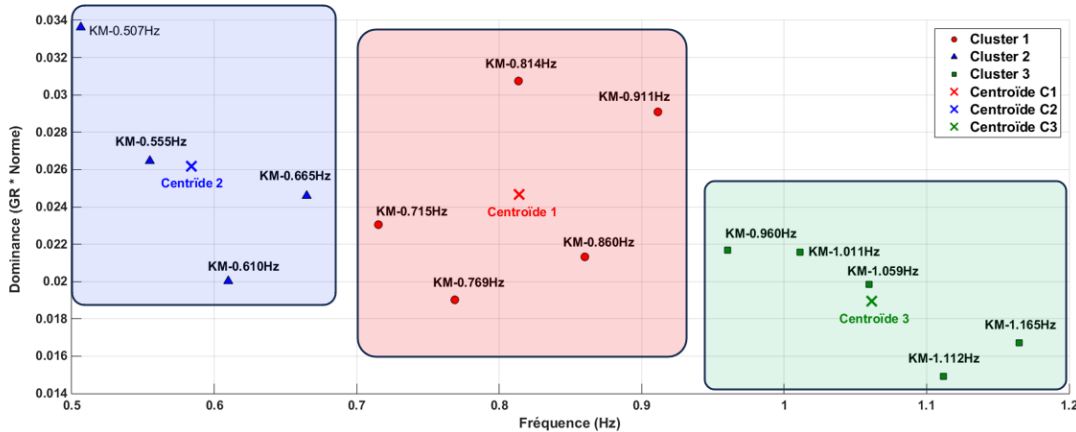


Figure 5: Automatic K-means Clustering of Koopman Mode

V. DISCUSSION

The oscillatory behavior of the Tunisian 2030 power system highlights structural patterns and nonlinear interactions that intensify with high renewable penetration. The combined use of Linear Modal Analysis (LMA) and Koopman Modal Analysis (KMA) provides complementary and consistent insights into these dynamics. At 35% RES penetration, reduced inertia and altered North–Centre–South power transfers increase the sensitivity of inter-area modes. KMA reveals additional nonlinear modes, particularly in the 0.5–0.81 Hz range, which are not captured by linear models, reflecting the growing complexity of system dynamics. Both LMA and KMA identify the North vs. [Centre + South] separation as the dominant inter-area pattern, with the 0.81 Hz mode becoming more pronounced under stressed North–South corridor conditions. KMA further shows that the inter-area response results from the interaction of multiple closely spaced modes, producing multi-frequency behavior and slow decay that LMA cannot resolve. Coherency analysis confirms the North as the main oscillatory block, the Centre as a dynamic buffer, and the South oscillating coherently with the Centre, with clustering techniques refining this structure for targeted damping strategies. While LMA remains valuable for small-signal modal identification, KMA enriches the analysis by capturing nonlinear dynamics, hidden modes, and long-term behavior. Together, they provide a comprehensive understanding of persistent oscillations and reveal key vulnerabilities related to reduced inertia and dependence on the North–South corridor, underscoring the need for reinforced networks and advanced control strategies.

VI. RECOMMENDATIONS FOR STABILITY ENHANCEMENT

Insights from LMA, KMA, time-domain simulations, and coherency analysis lead to targeted measures to improve the oscillatory stability of the Tunisian 2030 grid under high renewable penetration, addressing both control and structural aspects. Priority should be given to reinforcing damping through PSS installation or retuning on Northern generators, particularly the Rades (G2–G5) and BMC Zaghwén units (G6–G7), which dominate the critical 0.81 Hz mode. Tuning should focus on the 0.7–1 Hz band where inter-area and nonlinear modes are concentrated. In parallel, improved AVR/PSS coordination and supplementary damping control [16] on Central combined-cycle units (G10–G12) can strengthen their buffering role between North and South. Structural reinforcement of the 225/400 kV North–Centre–South corridor is essential to address the main system vulnerability, through line strengthening, additional transmission paths, enhanced reactive support, and increased short-circuit strength in the South. Given the nonlinear, multi-modal oscillations revealed by KMA, PMU-based wide-area monitoring and control at key nodes is recommended for early detection and mitigation of weakly damped modes [17]. Complementary operational measures—such as limiting sustained North–South transfers, maintaining balanced inertia, and ensuring adequate reserves—can further reduce oscillatory stress. Finally, the progressive deployment of grid-forming inverters [18], particularly in the Centre and South, offers a promising solution for providing synthetic inertia and enhancing long-term dynamic resilience.

VII. CONCLUSION

This book chapter presents a comprehensive assessment of the oscillatory stability of the Tunisian power system projected for 2030 under a peak-load scenario with 35% renewable energy penetration, using Linear Modal Analysis (LMA), Koopman Modal Analysis (KMA), and data-driven coherency methods. LMA identifies

a dominant inter-area mode around 0.8 Hz associated with North–Centre–South electromechanical interactions, while its linear formulation limits the representation of nonlinear and long-lasting dynamics typical of low-inertia systems. Koopman analysis reveals a richer modal structure, including weakly damped nonlinear modes in the critical 0.7–1.0 Hz band. The dominant Koopman mode at 0.814 Hz exhibits low damping and long decay times, and additional hidden modes highlight nonlinear interactions absent from the linear spectrum. Spatial Koopman mode shapes and coherency analysis consistently show the North as the most oscillatory region, the Centre as a stabilizing buffer, and the South swinging coherently with the Centre. These findings emphasize the structural influence of the transmission network and reduced inertia on inter-area oscillations, and support targeted damping improvements, reinforcement of the North–Centre–South corridor, wide-area PMU-based monitoring, and the adoption of grid-forming inverters. Overall, this chapter demonstrates that Koopman Modal Analysis is a powerful complement to classical modal techniques, providing deeper insight into nonlinear dynamics and coherency patterns essential for the secure operation of future renewable-dominated power systems.

ACKNOWLEDGMENT

The authors are grateful to Electrical Systems Laboratory of the National Engineering school of Tunis (ENIT) for supporting this work and providing the facilities needed to achieve this paper.

REFERENCES

- [1] I. Mezić, "Spectral properties of dynamical systems, model reduction and decompositions," *Nonlinear Dynamics*, vol. 41, pp. 309–325, 2005.
- [2] M. Budisić, R. Mohr, and I. Mezić, "Applied Koopmanism," *Chaos*, vol. 22, no. 4, 047510, 2012.
- [3] P. Kundur et al., *Power System Stability and Control*. McGraw-Hill, 1994.
- [4] S. L. Brunton et al., *Koopman Operator Theory for Dynamical Systems*. Cambridge Univ. Press, 2022.
- [5] T. Susuki and I. Mezić, "Nonlinear Koopman modes and coherency identification," *IEEE Trans. Power Syst.*, vol. 26, no. 4, pp. 1890–1901, 2011.
- [6] N. Takeishi, Y. Kawahara, "Learning Koopman invariant subspaces," *NIPS*, 2017.
- [7] S. Hassan et al., "Koopman-based modal analysis for renewable systems," *IEEE Access*, vol. 11, 2023.
- [8] L. Ju, H. Zhu, "Generator coherency from data-driven mode shapes," *IEEE Trans. Power Syst.*, vol. 37, no. 2, 2022.
- [9] J. Tu, C. Rowley, J. Kutz, "Dynamic Mode Decomposition," *J. Comput. Dyn.*, vol. 1, no. 2, 2014.
- [10] N. Takeishi and Y. Kawahara, "Data-Driven Spectral Analysis of Nonlinear Power System Dynamics Using Koopman Operators," *Electric Power Systems Research*, vol. 189, art. 106708, 2020.
- [11] Susuki, Y., Mezić, I. (2015). Nonlinear Koopman modes and coherency identification of coupled swing dynamics. *IEEE Transactions on Power Systems*, 31(2), 1191–1200, 2015.
- [12] Susuki, Y., Mezić, I., Hikihara, T. Coherent swing instability of power grids. *Journal of Nonlinear Science*, 21(3), 403–439, 2011.
- [13] Tantet, A., van der Weg, W., Dijkstra, H. A. Application of Koopman mode decomposition to the large-scale dynamics of electrical power grids. *Chaos*, 27(9), 093110, 2017.
- [14] Kutz, J. N., Brunton, S. L., Brunton, B. W., Proctor, J. L. *Dynamic Mode Decomposition: Data-Driven Modeling of Complex Systems*. SIAM, 2016.
- [15] Saha, S., Chowdhury, B. H. Dynamic modeling of renewable-integrated power systems using Koopman operator theory. *Electric Power Systems Research*, 189, 106750, 2020.
- [16] M. Bazrafshan, M. Gibbard, "Inter-area oscillations in low-inertia grids," *IEEE Trans. Power Syst.*, 2023.
- [17] T. Xia, G. Andersson, "Wide-area damping in renewable grids," *EPSR*, vol. 211, 2023.
- [18] Z. Wang et al., "Grid-forming inverters for oscillation damping," *IEEE Trans. Energy Conv.*, vol. 37, no. 4, 2022.